

## Regulation of L-type Calcium Channel Current by Somatostatin in Guinea-Pig Gastric Myocytes

Young Chul Kim, Jae Hoon Sim<sup>1</sup>, Sang Jin Lee, Tong Mook Kang<sup>2</sup>, Sung Joon Kim<sup>1</sup>, Seung Ryul Kim<sup>3</sup>, Sei Jin Youn<sup>4</sup>, Sang Jeon Lee<sup>5</sup>, Wen-Xie Xu<sup>6</sup>, Insuk So<sup>1</sup>, and Ki Whan Kim<sup>1</sup>

Department of Physiology, Chungbuk National University College of Medicine, Cheongju 361-763, <sup>1</sup>Department of Physiology and Biophysics, Seoul National University College of Medicine, Seoul 110-799, <sup>2</sup>Department of Physiology, Sungkyunkwan University School of Medicine, Suwon 440-746, Departments of <sup>3</sup>Biochemistry, <sup>4</sup>Internal Medicine, <sup>5</sup>Surgery, Chungbuk National University College of Medicine, Cheongju 361-763, <sup>6</sup>Department of Physiology, Medical School, Shanghai Jiao Tong University Shanghai, China

To study the direct effect of somatostatin (SS) on calcium channel current ( $I_{Ba}$ ) in guinea-pig gastric myocytes,  $I_{Ba}$  was recorded by using whole-cell patch clamp technique in single smooth muscle cells. Nifedipine (1  $\mu$ M), a L-type  $Ca^{2+}$  channel blocker, inhibited  $I_{Ba}$  by  $98 \pm 1.9\%$  ( $n=5$ ), however  $I_{Ba}$  was decreased in a reversible manner by application of SS. The peak  $I_{Ba}$  at 0 mV were decreased to  $95 \pm 1.1$ ,  $92 \pm 1.9$ ,  $82 \pm 4.0$ ,  $66 \pm 5.8$ ,  $10 \pm 2.9\%$  at  $10^{-10}$ ,  $10^{-9}$ ,  $10^{-8}$ ,  $10^{-7}$ ,  $10^{-5}$  M of SS, respectively ( $n=3-6$ ; mean  $\pm$  SEM). The steady-state activation and inactivation curves of  $I_{Ba}$  as a function of membrane potentials were well fitted by a Boltzmann equation. Voltage of half-activation ( $V_{0.5}$ ) was  $-12 \pm 0.5$  mV in control and  $-11 \pm 1.9$  mV in SS treated groups (respectively,  $n=5$ ). The same values of half-inactivation were  $-35 \pm 1.4$  mV and  $-35 \pm 1.9$  mV (respectively,  $n=5$ ). There was no significant difference in activation and inactivation kinetics of  $I_{Ba}$  by SS. Inhibitory effect of SS on  $I_{Ba}$  was significantly reduced by either dialysis of intracellular solution with GDP  $\beta$ S, a non-hydrolysable G protein inhibitor, or pretreatment with pertussis toxin (PTX). SS also decreased contraction of guinea-pig gastric antral smooth muscle. In conclusion, SS decreases voltage-dependent L-type calcium channel current (VDCC<sub>L</sub>) via PTX-sensitive signaling pathways in guinea-pig antral circular myocytes.

**Key Words:** Gastric myocytes, Calcium current, Somatostatin, G-protein

### INTRODUCTION

Since its initial isolation from the ovine, somatostatin (SS), tetradecapeptide, has been found in the central and peripheral nervous systems (Brazeau et al, 1983). SS is known to have a wide range of inhibitory actions as a hormone and a neurotransmitter in neural sites (Ertan et al, 1987). Within the gastrointestinal (GI) tract, SS is widely distributed in specific mucosa cells, on neurons in the mucosa and deeper level which project into smooth muscle cells (Arimura, 1975; Messenger, 1993). SS in GI tract is known to inhibit gastric endocrine and exocrine secretions in all species, and to reduce blood flow and absorptive activity (Gomez et al, 1975). With respect to GI motility, action of SS seems to be complex. SS inhibits migrating motor complexes in the stomach, but stimulates those in the intestine (Thor et al, 1978; Poitras et al, 1980). In longitudinal muscle of ileum, SS causes relaxation probably through inhibition of acetylcholine release (Teitelbaum et al, 1984). In addition to in vivo and tissue studies, the presence of somatostatin receptors (SSTRs) has been shown in many cell types, including guinea-pig gastric

smooth muscle cells by molecular cloning and ligand binding studies, and this implies that SS could play a local regulatory role in gastrointestinal tract (Sanders & Smith, 1986; Bell & Reisine, 1993; Gu et al, 1995; Corleto et al, 1997). In fact, SS inhibits agonist-induced contractions in colonic smooth muscle cells, but inhibits relaxation in gastric cells (Gu et al, 1992; Corleto et al, 1997). Therefore, the effect of SS on calcium channels should be investigated.

Dihydropyridine-sensitive voltage-dependent L-type  $Ca^{2+}$  channels (VDCC<sub>L</sub>) have been described in most excitable tissues, including guinea-pig gastric circular myocyte (Hagiwara & Byerly, 1981; Katzka & Morad, 1989), and VDCC<sub>L</sub> are known to play a central role in the regulation of  $[Ca^{2+}]_i$  in smooth muscles (Kim et al, 1997). In addition, the contractile activity of GI smooth muscles is closely related to electrical autorhythmicity which is termed as slow wave, and the activation of plateau  $Ca^{2+}$  current is necessary for excitation-contraction coupling (Barajas & Huizinga, 1986). Generally, calcium channels in smooth muscles are known to be regulated by many factors such as a wide variety of neurotransmitters, intracellular cyclic nucleotides (cAMP, cGMP), stretch (cytoskeleton), and so on (Xiong et al, 1994; Koh & Sanders, 1996; Xu et al, 1996). Neuropeptide and neurotransmitters such as vasoactive intestinal peptide

Corresponding to: Young Chul Kim, Department of Physiology, Chungbuk National University College of Medicine, 12 Gaeshindong, Heungduk-gu, Cheongju 361-763, Korea. (Tel) 82-43-261-2859, (Fax) 82-43-261-2859, (E-mail) physiokyc@chungbuk.ac.kr

**ABBREVIATIONS:** SS, somatostatin;  $I_{Ba}$ , calcium channel current; PTX, pertussis toxin; VDCC<sub>L</sub>, L-type calcium channel current.

(VIP), acetylcholine (ACh) and norepinephrine (NE) are also known to regulate  $\text{Ca}^{2+}$  current of smooth muscle including gastrointestinal smooth muscle, through cyclic nucleotide and protein kinase (Kamimura N et al, 1996; Koh & Sanders, 1996; Wade GR et al, 1996; Seki T et al, 1999).

Effects of SS on VDCC in several types of neural cells have been reported (Chen et al, 1989; Ikeda & Schofield, 1989). The mechanism underlying regulation of calcium current by SS in neuronal cells has been suggested to be responsible for activation of pertussis toxin (PTX) sensitive G protein (Ikeda & Schofield, 1989; Hill, 1992). And the effects of SS on calcium current are reversible and concentration-dependent inhibitory (Ikeda & Schofield, 1989; Meriney et al, 1995). In cardiac cells, inhibitory effect of SS on L-type calcium current and  $\text{Ca}^{2+}$  influx through calcium channels was also reported in guinea-pig atrium (Diez J & Tamargo J, 1987; Ohmura T et al, 1990). Even though the inhibitory effect of SS on vasoactive intestinal peptide (VIP)-induced relaxation through Gi protein in dispersed gastric smooth muscle cells was reported, no direct effect of SS on ionic current in GI smooth muscle cells has yet been reported (Gu et al, 1992). Therefore, the aim of this experiment was to investigate the effect of SS on  $\text{Ca}^{2+}$  channel in guinea-pig gastric myocytes and its possible mechanism.

## METHODS

### Preparation of cells

Guinea-pigs of either sex, weighing 300–350 g, were exsanguinated after stunning. The antral portion of stomach was cut, and the mucosal layer was separated from the muscle layers in  $\text{Ca}^{2+}$ -free physiological salt solution ( $\text{Ca}^{2+}$ -free PSS). The circular muscle layer was dissected from the longitudinal layer using fine scissors and made into small segments ( $2 \times 3$  mm). These segments were incubated in  $\text{Ca}^{2+}$ -free PSS for 30 min at  $4^\circ\text{C}$ . Then, they were incubated for 15–25 min at  $35^\circ\text{C}$  in the digestion medium containing 0.1% collagenase (Wako, Japan), 0.05% dithioerythritol, 0.1% trypsin inhibitor and 0.2% bovine serum albumin. After digestion, the supernatant was discarded, and the softened muscle segments were transferred into modified Kraft-Brühe (K-B) medium (Isenberg & Klöckner, 1982). And single cells were then dispersed by gentle agitation with a wide-bore glass pipette. Isolated gastric myocytes were kept in K-B medium at  $4^\circ\text{C}$  until use. All experiments were carried out within 8 hours of harvesting cells and performed at room temperature.

### Whole-cell voltage clamp

Isolated cells were transferred to a small chamber on the stage of an inverted microscope (IMT-2, Olympus, Japan). The chamber was perfused with PSS (2–3 ml/min). Glass pipettes with a resistance of 2–5 M $\Omega$  were used to make a giga seal of 5–10 G $\Omega$ . Standard patch clamp techniques were used (Hamill et al, 1981). An axopatch-1C patch-clamp amplifier (Axon instruments, USA) was used to record membrane currents, and command pulses were applied by using IBM-compatible AT computer and pClamp software v.5.5.1. The data were displayed on a digital oscilloscope and a computer monitor.

### Preparation of muscle strips and conventional intracellular recording

A horizontal chamber of 2 ml in the capacity was used for the experiment, where continuous solution exchange was needed (2–3 ml/min). The muscle strips ( $5 \times 5$  mm) from the proximal part of antrum were cut parallel to circular fibers and mounted on a silicon rubber with pins in a 2 ml horizontal chamber. The strip was constantly perfused at a rate of 2–3 ml/min with  $\text{CO}_2$ /bicarbonate-buffered Tyrode solution ( $36^\circ\text{C}$ ). For the recording of electrical activity, glass microelectrode was prepared by PUL-1 (World Precision Instruments, USA) and filled with 3 M KCl (tip resistance of 40–80 M $\Omega$ ). Finally, electrical activity of tissue was recorded using intracellular electrometer (IE-201, Warner Instrument Corporation, USA) and drawn by a chart recorder (Gould, USA) and computer. For measurement of isometric contraction, vertical chamber and force transducer were used.

### Solution and drugs

$\text{Ca}^{2+}$ -free PSS, containing (in mM): NaCl 135, KCl 5,  $\text{CaCl}_2$  1.8,  $\text{MgCl}_2$  1, glucose 10, and HEPES (*N*-[2-hydroxyethyl] piperazine-*N*-[2-ethanesulphonic acid]) 10, was adjusted to pH 7.4 with NaOH. Modified K-B solution, containing (mM) L-glutamate 50, KCl 50, taurine 20,  $\text{KH}_2\text{PO}_4$  20,  $\text{MgCl}_2$  3, glucose 10, HEPES 10, ethyleneglycol bis-( $\beta$ -aminoethyl ether-*N,N,N,N*-tetraacetic acid (EGTA) 0.5, was adjusted to pH 7.4 with KOH. Pipette solution, containing (mM) CsCl 110, TEA 20, EGTA 10, HEPES 10,  $\text{Na}_2\text{ATP}$  3,  $\text{MgCl}_2$  3.5, was adjusted to pH 7.3 with TRIZMA or CsOH. Phosphate-buffered Tyrode solution contained (in mM) NaCl 147, KCl 4,  $\text{MgCl}_2$  1,  $\text{CaCl}_2$  1.8,  $\text{NaH}_2\text{PO}_4$  0.42,  $\text{Na}_2\text{HPO}_4$  1.81, and glucose 5.5 (pH 7.3).  $\text{CO}_2$ /bicarbonate-buffered Tyrode solution contained (in mM) NaCl 122, KCl 4.7,  $\text{MgCl}_2$  1,  $\text{CaCl}_2$  2,  $\text{NaHCO}_3$  15,  $\text{KH}_2\text{PO}_4$  0.93, and glucose 11 (pH 7.3–7.4, bubbled with 5%  $\text{CO}_2$ /95%  $\text{O}_2$ ). All drugs used in this study were purchased from Sigma.

### Statistics

The data are expressed as means  $\pm$  SEM. Statistical significance was estimated by paired and unpaired Student's *t*-test.  $p < 0.05$  was considered to be statistically significant.

## RESULTS

### Effects of SS on the voltage activated calcium channel current ( $I_{\text{Ba}}$ )

Extracellular  $\text{Ca}^{2+}$  was replaced by 10 mM  $\text{Ba}^{2+}$ , and membrane potential was held at  $-80$  mV. Step to 0 mV for 320 msec from  $-80$  mV was applied to cells at every 15 sec to record  $I_{\text{Ba}}$ . Effect of SS on  $I_{\text{Ba}}$  at 0 mV was studied before and after application of SS to bath solution. Ten nM SS decreased  $I_{\text{Ba}}$  at 0 mV in a reversible manner and representative raw current traces are shown in Fig. 1A. In Fig. 1B, peak values of  $I_{\text{Ba}}$  were plotted as a function of time during the application of SS. Reversible and inhibitory effect of SS (10 nM) on  $I_{\text{Ba}}$  is shown. Current/voltage relationship of  $I_{\text{Ba}}$  was studied in the absence and presence

of SS (Fig. 1C). The membrane potential was held at  $-80$  mV, and  $10$  mV step depolarization, ranging from  $-40$  mV to  $+50$  mV, were applied to cell for  $320$  ms before and after application of SS. Normalized responses obtained at  $0$  mV against the peak value were averaged and plotted (Closed circle Control, closed uptriangle  $10$  nM SS). And  $10$  nM SS decreased  $I_{Ba}$  at membrane potential range of  $-20 \sim +40$  mV tested ( $n=5$ ;  $p < 0.05$ ). Various concentrations of SS on peak value of  $I_{Ba}$  at  $0$  mV was studied, and the result is shown in Fig 2. Peak values of  $I_{Ba}$  at  $0$  mV were significantly decreased to  $95 \pm 1.1$ ,  $92 \pm 1.9$ ,  $82 \pm 4.0$ ,  $66 \pm 5.8$ ,  $10 \pm 2.9\%$  at  $10^{-10}$ ,  $10^{-9}$ ,  $10^{-8}$ ,  $10^{-7}$ ,  $10^{-5}$  M SS, respectively, compared to control (mean SEM,  $n=3 \sim 6$ ;  $p < 0.05$ ;  $IC_{50}=140$  nM).

### Effect of SS on steady-state activation and inactivation of $I_{Ba}$

A modified double-pulse protocol was used to measure the steady-state inactivation of  $I_{Ba}$  as a function of membrane potentials. Prepulse potential, ranging from  $-100$  to  $+20$  mV, were applied for a duration of  $3.75$  sec. Following a  $7$  msec interpulse interval at a potential of  $-60$  mV, the membrane potential was raised to a test potential of  $0$  mV for  $1$  sec. The currents were then normalized to the current obtained at  $-100$  mV ( $I/I_{max}$ ) and plotted against each pre-

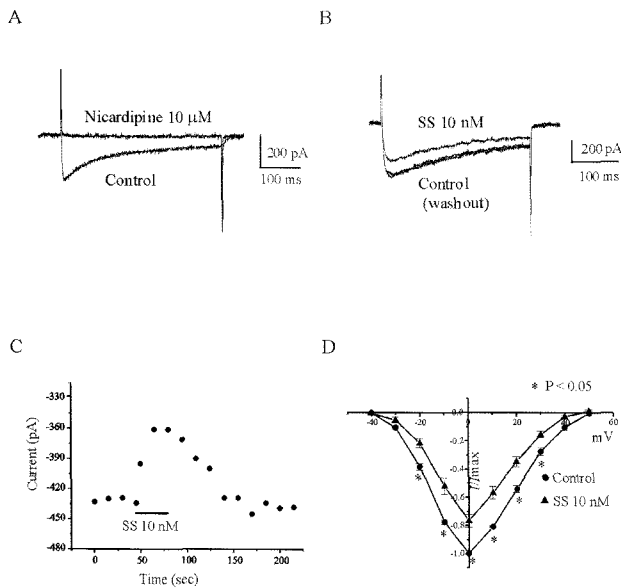


**Fig. 1.** Effect of SS on  $I_{Ba}$ .  $I_{Ba}$  was recorded under the condition in which extracellular  $Ca^{2+}$  was replaced by  $10$  mM  $Ba^{2+}$ . In A, raw trace of  $I_{Ba}$  blocked by  $1$  mM nicardipine is shown.  $I_{Ba}$  was decreased by SS and returned to control level by washout in B. In C, peak values of  $I_{Ba}$  were plotted as a function of time in the presence and absence of SS. SS ( $10$  nM) inhibited  $I_{Ba}$  in a reversible manner. Current/voltage relationship of  $I_{Ba}$  by SS is shown in D. Normalized responses against the peak value obtained at  $0$  mV were averaged and plotted ( $n=5$ ; Closed circle Control, closed uptriangle  $10$  nM SS).

pulse potential. Plotted data were well fitted by a Boltzmann equation, with a half-inactivation voltage ( $V_{0.5}$ ) of  $-35 \pm 1.4$  mV in control and  $-35 \pm 1.9$  mV in SS treated groups ( $n=5$ ), and slope factor ( $k$ ) of  $13 \pm 1.1$  in control and  $14 \pm 1.3$  in SS treated cells ( $n=5$ ; Fig. 3;  $p > 0.05$ ). Steady-state activation curves were estimated from the I/V relations of  $I_{Ba}$  in the presence and absence of  $10$  nM SS. The peak conductance at each potential was calculated by using the following equation:  $I_{Ba} = g_{Ba} \times (V - E_{rev})$  where  $g_{Ba}$ ,  $V$ , and  $E_{rev}$  are peak conductance, test potential and observed reversal potential, respectively. The values of half-activation were  $-12 \pm 0.5$  mV and  $-11 \pm 1.9$  mV ( $n=5$ , respectively) with slope factors ( $k$ ) of  $6 \pm 0.6$  and  $5 \pm 0.2$  in control and SS treated groups, respectively ( $n=5$ ; Fig. 3;  $p > 0.05$ ).

### Effect of SS on $I_{Ba}$ in the presence of $GDP\beta S$

It is well known that SS inhibits  $I_{Ca}$  via G-protein mediated pathway in neuronal cells. Therefore, we tried to elucidate whether the PTX-sensitive G-protein mediates

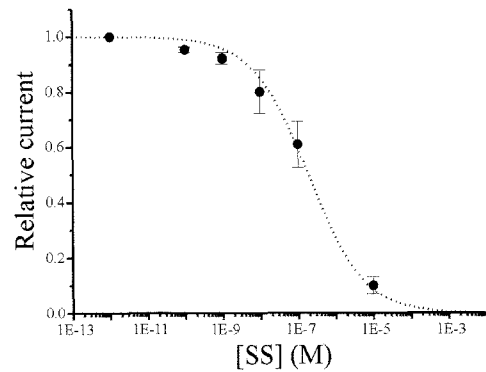


**Fig. 2.** Concentration-response relationship of SS. When SS was applied to the bath solution,  $I_{Ba}$  at  $0$  mV was decreased by SS ( $1$  pM  $\sim 10$   $\mu$ M) in a reversible manner. Relative currents at various concentration of SS are plotted and fitted by the non-linear regression equation (mean  $\pm$  SEM,  $n=3 \sim 6$ ).

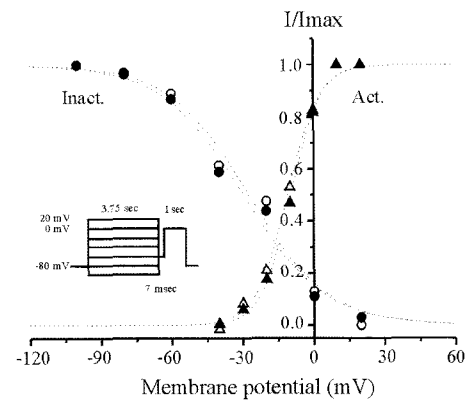


**Fig. 3.** Effects of SS on steady-state activation and inactivation curves of  $I_{Ba}$ . Steady-state activation and inactivation curves for the cells exposed to control ( $\blacktriangle$ ,  $\bullet$ ) and SS treated cells ( $\triangle$ ,  $\circ$ ). There were no significant difference in values of half-activation, halfinactivation and slope factors ( $k$ ) between control and SS treated groups ( $n=5$ ,  $p > 0.05$ ).

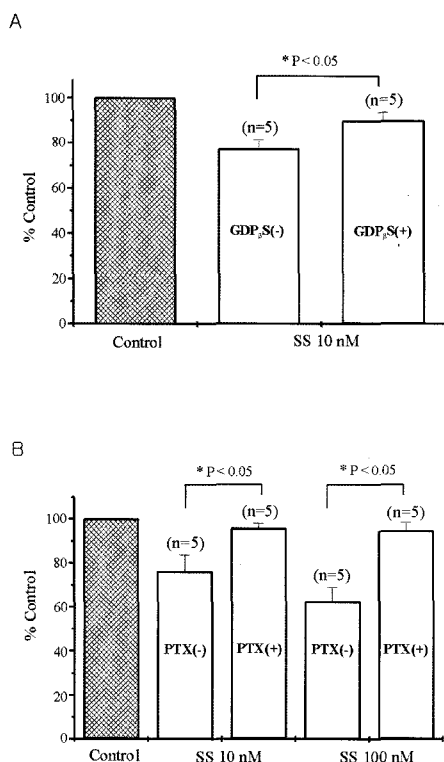


**Fig. 4.** Effects of GDP $\beta$ S and PTX on SS-induced inhibition of  $I_{Ba}$ . (A) The inhibitory effect of SS on  $I_{Ba}$  was significantly suppressed after 10 min of cytosolic dialysis with GDP $\beta$ S (5 mM) through pipette solution ( $n=5$ ,  $p<0.05$ ). (B) Inhibitory effect of SS on  $I_{Ba}$  was significantly suppressed by pre-treatment with PTX for 6 hours ( $n=5$ ,  $p<0.05$ ).

the inhibitory effect of SS on  $I_{Ba}$ . As a first step, the effect of non-hydrolysable analog, guanosine 5-O- $\beta$ -thio diphosphate (GDP $\beta$ S), on SS-induced inhibition of  $I_{Ba}$  was studied (Fig. 4A). GDP $\beta$ S (5 mM) in the pipette solution was dialysed for 10 min via breakthrough the patch membrane. When SS was perfused to the bath solution after 10 min of internal dialysis of GDP $\beta$ S, decreasing effect of SS on  $I_{Ba}$  was significantly reduced ( $n=5$ ; Fig. 4A;  $p<0.05$ ). In GDP $\beta$ S treated groups, SS decreased  $I_{Ba}$  to  $78\pm 3.8\%$ , compared to control groups ( $89\pm 3.8\%$ ). For PTX pre-treatment, dissociated antral gastric smooth muscle cells were incubated with PTX ( $2\ \mu\text{g/ml}$ ) for 6 hours at  $37^\circ\text{C}$ . And control cells were incubated at the same temperature with normal solution including 1 mg of BSA. When cells was incubated with PTX at  $37^\circ\text{C}$ , inhibitory effects of 10 and 100 nM SS on  $I_{Ba}$  were significantly reduced ( $n=5$ , Fig. 4B;  $p<0.05$ ). In PTX pretreated groups, 10 and 100 nM SS reduced  $I_{Ba}$  to  $95\pm 2.1$  and  $94\pm 3.6\%$  ( $n=5$ , respectively), compared to control ( $76\pm 7.5$  and  $63\pm 6.4$ ;  $n=5$ , respectively).

#### Effect of SS on slow wave and contraction of guinea-pig gastric antral smooth muscle

Resting membrane potential (RMP), frequency, amplitude and slope of slow wave in the absence of SS were  $-62\pm 1.1$  mV,  $3.2\pm 0.3$  cycle/min,  $30\pm 1.0$  mV and  $0.13\pm 0.01$  V/sec, respectively. No significant changes of these factors

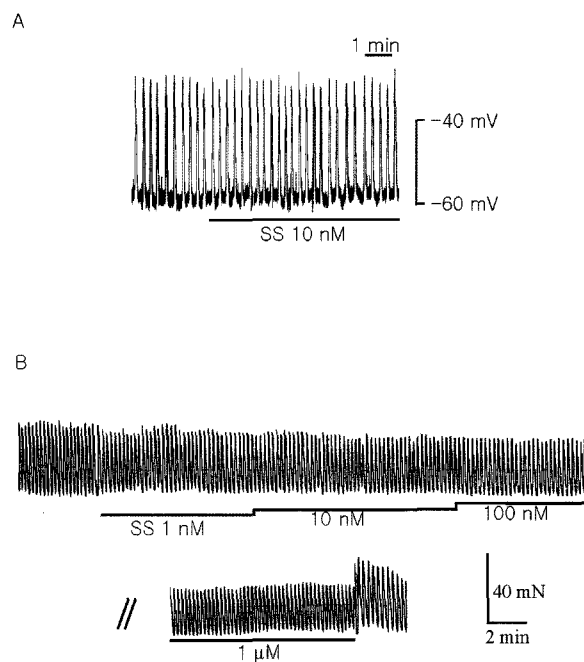


**Fig. 5.** Effects of SS on slow wave and contraction in guinea-pig gastric circular smooth muscle. (A) Membrane potential was recorded using conventional intracellular recording, and effects of 10 nM SS on slow wave were studied. SS did not show any significant effect on slow wave in guinea-pig gastric circular smooth muscle ( $n=5$ ,  $p>0.05$ ). (B) Effects of SS on contraction in guinea pig gastric antral circular smooth muscle were studied. SS (1 nM– $1\ \mu\text{M}$ ) decreased contraction.

were observed in the presence or absence of 10 nM SS. In the presence of 10 nM SS, the above values were  $-61\pm 0.9$  mV,  $3.0\pm 0.3$  cycle/min,  $28\pm 0.9$  mV and  $0.13\pm 0.01$  V/sec, respectively ( $n=5$ ; Fig. 5A;  $p>0.05$ ). Effect of SS on isometric contraction of guinea-pig gastric antral smooth muscle was studied. In four strips tested, 1 nM, 10 nM, 100 nM and  $1\ \mu\text{M}$  SS decreased the contraction by  $12\pm 7.3$ ,  $18\pm 13$ ,  $20\pm 12$ , and  $24\pm 14\%$  of the control, respectively ( $n=4$ ; Fig. 5B).

## DISCUSSION

Voltage-dependent  $\text{Ca}^{2+}$  channel (VDCC) in gastrointestinal (GI) tract plays an important role in the regulation of  $[\text{Ca}^{2+}]_i$  and contraction, including slow wave (Bauer & Sanders, 1985; Barajas & Huizinga, 1986; Sanders & Smith, 1986; Kim et al, 1997; Kim et al, 2002). Especially, slow wave is a fundamental property in GI tract and is essential for normal GI motility. This event regulates the phasic contractions of the gut. Many studies indicate that the interstitial cells of Cajal (ICC) are the pacemaker cells that generate slow wave (Ward et al, 1994; Huizinga, 1995; Kito & Suzuki, 2003). Recently, VDCCs in ICC of murine GI tract were identified, and the propagation of slow wave by  $\text{Ca}^{2+}$  entry through VDCC in ICC has been reported (Kim et al, 2002; Ward et al, 2004). Therefore, identification and elucidation of regulatory factors of VDCC in smooth muscle and ICC of GI tract appear to be very important. GI motility and slow wave are also regulated by many neurotransmit-

ters, including neuropeptides. And SS is also found in GI tract, however, the role of SS in  $I_{Ba}$  of GI has not yet been studied (Arimura, 1975; Mihara & North, 1987b; Bell & Reisine, 1993).

In this study, we tried to elucidate the effect of SS on VDCC of guinea-pig gastric myocytes. As shown in Fig. 1 and 2, we found inhibitory effect of SS on  $I_{Ba}$  in guinea-pig gastric myocytes: SS significantly reversibly decreased  $I_{Ba}$  in a concentration dependent manner (Fig. 2). These effects are very similar to the effect of SS on cardiac and neuronal cell: In neuronal cell, SS ( $10^{-10}$ – $10^{-6}$  M) inhibits VDCC (Ikeda & Schofield, 1989), and SS also decreased L-type  $Ca^{2+}$  current in cardiac myocytes in a reversible manner (Diez J & Tamargo J, 1987; Ohmura T et al, 1990). In these reports, SS was shown to selectively reduce  $Ca^{2+}$  current without affecting  $Na^+$  and  $K^+$  current. The effect of SS to reduce  $Ca^{2+}$  current in cardiac myocytes was responsible for negative inotropic effect (Ohmura T et al, 1990).

The effect of SS on steady-state activation and inactivation curves of  $I_{Ba}$  is shown in Fig. 3. Steady-state activation and inactivation curves were well fitted by a Boltzmann equation as a function of membrane potentials. However, there was no significant differences in half-activation and -inactivation values between control and SS treated groups (Fig 3,  $p > 0.05$ ). In addition, intracellular application of  $GDP_{\beta}S$  which is known to compete with GTP for binding, and pretreatment of PTX significantly reduced the effect of SS on  $I_{Ba}$  (Fig. 4). To the best of our knowledge, there has been no report about G-protein involved in inhibitory regulation of  $Ca^{2+}$  channels by SS in gastrointestinal tract. Generally, G-proteins couple variety of plasma membrane receptors to VDCCs: For example, it directly or indirectly activates VDCCs via cytoplasmic second messengers (Holz, 1986; Lewis et al, 1986). The results presented in this study led us to suggest that PTX-sensitive G-protein, which is also known to be involved in signal transduction, mediated regulation of  $I_{Ba}$  in guinea-pig gastric myocytes.

In this study, we also tried to elucidate the effect of SS on slow wave in guinea-pig gastric antral smooth muscle. In GI tract, blockers of VDCC, such as verapamil and diltiazem, are known to reduce of maximum rate of rise (dV/dT) of slow wave (Ishikawa et al, 1985). As shown in Figs. 1 and 2, we found inhibitory effect of SS on  $I_{Ba}$  in guinea-pig gastric myocyte. However, 10 nM SS did not show significant effect on the slope of initial portion of slow wave (Fig. 5A). Even though not shown, 100 nM SS also showed significant effect on the slope of slow wave. Slopes before and after the treatment of SS were  $0.13 \pm 0.03$  V/sec and  $0.1 \pm 0.01$  V/sec, respectively ( $n=3$ ,  $p > 0.05$ ). In general, SS is known to be an inhibitory peptide in some GI smooth muscles, including vascular smooth muscle (Corleto et al, 1997; Ruiz E et al, 2002). Since we suggested inhibitory effect of SS on calcium current in GI tract, these mechanisms might be related to relaxation of smooth muscle. To study this possibility, we tried to study the effect of SS on contraction in guinea-pig antral circular muscle. As shown in Fig. 5B, SS decreased contractions of antral circular muscle, thus supporting the notion that SS might play an inhibitory role in GI smooth muscle (Corleto et al, 1997). However, higher concentration of SS than that of SS on  $I_{Ba}$  was applied to the bath solution in order to achieve inhibitory action of SS on contraction. In fact, concentrations of SS on the cell directly and deeper level in tissue might be different. Therefore, there is a possibility that efficiencies of SS on  $I_{Ba}$  in a single cell and contraction,

including slow wave, in tissue level might be somewhat different.

Finally, we investigated the effect of SS on voltage dependent  $K^+$  current ( $I_{Kdr}$ ). Many studies have already reported that electrical effects of SS appear to be mediated by  $K^+$  conductance which produce hyperpolarization in mammalian CNS neurons (Mueller et al, 1986; Pittman & Siggins, 1991). Similar results were also reported in guinea-pig submucosa plexus neurons, including GH3 pituitary cells, and attributed to activation of inwardly rectifying  $K^+$  channel (Mihara & North, 1987b). Therefore, we also studied the effect of SS on  $I_{Kdr}$  in guinea-pig gastric myocytes. When SS was applied 5 min before recording this current, outward current was not significantly affected, compared to control (data not shown,  $n=5$ ,  $p > 0.05$ ). That implies that SS may have selective effect on the regulation of calcium current rather than  $K^+$  channels in guinea-pig gastric myocytes.

In summary, this study provides evidence that SS decreased  $I_{Ba}$  in concentration- and voltage-independent manner, and its underlying mechanism responsible for decreasing  $I_{Ba}$  is the activation of PTX-sensitive G-protein in guinea-pig gastric myocytes.

## ACKNOWLEDGEMENT

This work was supported by BumSuk Academic Research Fund of 2003.

## REFERENCES

- Arimura A, Sato H, Dupont A, Nishi N, Schally AV. Somatostatin: abundance of immunoreactive hormone in rat stomach and pancreas. *Science* 189: 1007–1009, 1975
- Barajas-Lopez C, Huizinga JD. Different mechanisms of contraction generation in canine colon. *Am J Physiol* 256: G570–G580, 1986
- Bauer AJ, Sanders KM. Gradient in excitation-contraction coupling in canine gastric antral circular muscle. *J Physiol* 369: 283–294, 1985
- Bell GI, Reisine T. Molecular biology of somatostatin receptors. *Trends Neuro Sci* 16: 34–38, 1993
- Brazeau P, Vale W, Burgus R, Ling N, Butcher M, Rivier J, Guillemin R. Hypothalamic polypeptide that inhibits the secretion of immunoreactive pituitary growth hormone. *Science* 179: 77–79, 1973
- Chen C, Israel JM, Vincent JD. Electrophysiological responses to somatostatin of rat hypophysial cells in somatotroph-enriched primary cultures. *J Physiol* 408: 493–510, 1989
- Corleto VD, Severi C, Coy DH, Delle Fave G, Jensen RT. Colonic smooth muscle cells possess a different subtype of somatostatin receptor from gastric smooth muscle cells. *Am J Physiol* 272: G689–697, 1997
- Diez J, Tamargo J, Valenzuela C. Negative effect of somatostatin in guinea-pig atrial fibres. *Br J Pharmacol* 86: 547–555, 1985
- Ertan A, Arimura A. Somatostatin and the stomach. *Dig Dis Sci* 5: 13–20, 1987
- Gomez-Pan A, Reed JD, Albinus M, Shaw B, Hall R, Besser GM, Coy DH, Kastin AJ, Schally AV. Direct inhibition of gastric acid and pepsin secretion by growth hormone-release inhibiting hormone in cats. *Lancet* 1: 888–890, 1975
- Gu ZF, Pradhan T, Coy DH, Mantey SA, Bunnett NW, Jensen RT, Maton PN. Actions of somatostatins on gastric smooth muscle cells. *Am J Physiol* 262: G432–G438, 1992
- Gu ZF, Corleto VD, Mantey SA, Coy DH, Maton PN, Jensen RT. Somatostatin receptor subtype 3 mediates the inhibitory action of somatostatin on gastric smooth muscle cells. *Am J Physiol* 268: G739–G748, 1995
- Hagiwara S, Byerly L. Membrane biophysics of calcium channels.

- Fed Proc* 40: 2220–2225, 1981
- Hamill OP, Marty A, Neher E, Sakmann B, Sigworth FJ. Improved patch-clamp techniques for high resolution current recording from cells and cell-free membrane patches. *Pflügers Arch-Eur J Physiol* 391: 85–100, 1981
- Hill B. G protein-coupled mechanisms and nervous signaling. *Neuron* 9: 187–195, 1992
- Holz GG, Rane SG, Dunlap K. GTP-binding proteins mediate transmitter inhibition of voltage-dependent calcium channels. *Nature* 319: 670–672, 1986
- Huizinga, JD, Thuneberg L, Klüppel M, Malysz J, Mikkelsen HB, Bernstein A. *W*/kit gene required for intestinal pacemaker activity. *Nature* 373: 347–349, 1995
- Ikeda SR, Schofield GG. Somatostatin blocks a calcium current in rat sympathetic ganglion neurons. *J Physiol* 409: 221–240, 1989
- Isenberg G, Klöckner U. Calcium tolerant ventricular myocytes prepared by pe-incubation in a K-B-medium. *Pflügers Arch-Eur J Physiol* 424: 431–438, 1982
- Ishikawa S, Komori K, Nagao T, Suzuki H. Effects of diltiazem on electrical responses evoked spontaneously or by electrical stimulation in the antrum smooth muscle cells of the guinea-pig stomach. *Br J Pharmacol* 86: 789–797, 1985
- Kamimura N, Suga S, Wada J, Mio Y, Suzuki T, Wakui M. Excitatory and inhibitory actions of norepinephrine on the Ba<sup>2+</sup> current through L-type Ca<sup>2+</sup> channels of smooth muscle cells of guinea-pig vas deferens. *J Cell Physiol* 169: 373–379, 1996
- Katzka DA, Morad M. Properties of calcium channels in guinea-pig gastric myocytes. *J Physiol* 413: 175–197, 1989
- Kim SJ, Ahn SC, Kim JK, Kim YC, So I, Kim KW. Changes in intracellular Ca<sup>2+</sup> concentration induced by L-type Ca<sup>2+</sup> channel current in guinea-pig gastric myocytes. *Am J Physiol* 8273: C1947–1956, 1997
- Kim YC, Koh SD, Sanders KM. Voltage-dependent inward currents of interstitial cells of Cajal from murine colon and small intestine. *J Physiol* 541(Pt 3): 797–810, 2002
- Kito Y, Suzuki H. Properties of pacemaker potentials recorded from myenteric interstitial cells of Cajal distributed in the mouse small intestine. *J Physiol* 553(Pt 3): 803–818, 2003
- Koh SD, Sanders KM. Modulation of Ca<sup>2+</sup> current in canine colonic myocytes by cyclic nucleotide-dependent mechanisms. *Am J Physiol* 271: C794–C803, 1996
- Lewis DL, Weight FF, Luini A. A guanine nucleotide-binding protein mediates the inhibition of voltage-dependent calcium current by somatostatin in a pituitary cell line. *Proc Natl Acad Sci* 83: 9035–9039, 1986
- Meriney SD, Gray DB, Pilar GR. Somatostatin-induced inhibition of neuronal Ca<sup>2+</sup> current modulated by cGMP-dependent protein kinase. *Nature* 369: 336–339, 1995
- Messenger JP. Immunohistochemical analysis of neurons and their projections in the proximal colon of the guinea-pig. *Arch Histol Cytol* 56: 459–473, 1993
- Mihara S, North RA, Surprenant A. Somatostatin increases an inwardly rectifying potassium conductance in guinea-pig submucous plexus neurones. *J Physiol* 390: 335–355, 1987b
- Mueller AL, Kunkel DD, Schwartzkroin PA. Electrophysiological actions of somatostatin (SRIF) in hippocampus: an in vitro study. *Cell Mol Neurobiol* 6: 363–379, 1986
- Ohmura T, Nishio M, Kigoshi S, Muramatsu I. Somatostatin decreases the calcium inward current in guinea-pig atria. *Br J Pharmacol* 99: 587–591, 1990
- Pittman QJ, Siggins GR. Somatostatin hyperpolarizes hippocampal pyramidal cells in vitro. *Brain Res* 221: 402–408, 1991
- Poitras P, Steinbach JH, Vandeventer G, Code CF, Walsh JH. Motilin-independent ectopic fronts of the interdigestive myoelectric complex in dog. *Am J Physiol* 239: 215–220, 1980
- Raynor K, O'Carroll AM, Kong H, Yasuda K, Mahan LC, Bell GI, Reisine T. Characterization of cloned somatostatin receptors SSTR4 and SSTR5. *Mol Pharmacol* 44: 385–392, 1993
- Ruiz E, Padilla E, Tejerina T. Effect of somatostatin on rabbit coronary arteries. *Jpn J Pharmacol* 90: 51–58, 2002
- Sanders KM, Smith TK. Motoneurons of the submucous plexus regulate electrical activity of the circular muscle of the canine proximal colon. *J Physiol* 380: 293–310, 1986
- Seki T, Yokoshiki H, Sunagawa M, Nakamura M, Sperelakis N. Angiotensin II stimulation of Ca<sup>2+</sup> current in vascular smooth muscle cells is inhibited by lavendustin-A and LY-294002. *Pflügers Arch* 437: 317–323, 1999
- Teitelbaum DH, O'Doriso TM, Perkins WE, Gaginella S. Somatostatin modulation of peptide-induced acetylcholine release in guinea-pig ileum. *Am J Physiol* 246: G509–G514, 1984
- Thor P, Krol R, Konturek SJ, Coy DH, Schally AV. Effect of somatostatin on myoelectrical activity of small bowel. *Am J Physiol* 235: E249–E254, 1978
- Wade GR, Barbera J, Sims SM. Cholinergic inhibition of Ca<sup>2+</sup> current in guinea-pig gastric and tracheal smooth muscle cells. *J Physiol* 491: 307–319, 1996
- Ward SM, Bums AJ, Torihashi S, Sanders KM. Mutation of the proto-oncogene c-kit development of interstitial cells and electrical rhythmicity in murine intestine. *J Physiol* 480: 91–97, 1994
- Ward SM, Dixon RE, De Faoite A, Sanders KM. Voltage-dependent calcium entry underlies propagation of slow waves in canine gastric antrum. *J Physiol* 561: 793–810, 2004
- Yatani A, Codina J, Brown AM, Birnbaumer L. Direct activation of mammalian atrial muscarinic potassium channels by GTP regulatory protein Gk. *Science* 235: 207–211, 1987
- Xiong Z, Sperelakis N, Fenoglio-Preiser C. Regulation of L-type calcium channels by cyclic nucleotides and phosphorylation in smooth muscle cells from rabbit portal vein. *J Vasc Res* 31: 271–279, 1994
- Xu WX, Kim SJ, Kim SJ, So I, Kang TM, Rhee JC, Kim KW. Effect of stretch on calcium channel currents recorded from the antral circular myocytes of guinea-pig stomach. *Pflügers Arch-Eur J Physiol* 432: 159–164, 1996